# Unraveling Anhydrous Proton Conduction in Hydroxygraphane

Abhishek Bagusetty<sup>†,‡</sup> and J. Karl Johnson\*,‡

†Computational Modeling & Simulation Program, University of Pittsburgh, Pittsburgh PA 15260, USA

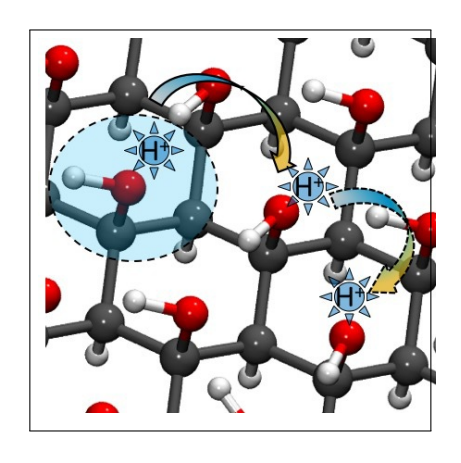
‡Department of Chemical & Petroleum Engineering, University of Pittsburgh, Pittsburgh PA 15261, USA

E-mail: karlj@pitt.edu

#### Abstract

We predict that graphane functionalized with hydroxyl groups, hydroxygraphane, can conduct protons in the complete absence of water, as shown from density functional theory calculations. Hydroxygraphane's anhydrous intrinsic proton conductivity results from the selfassembling two-dimensional network of hydrogen bonds on its surface. We show that the proton conduction occurs through a Grotthusslike mechanism, as protons hop between neighboring hydroxyl groups, aided by their rotation. Our calculations predict that hydroxygraphane has a direct bandgap of 3.43 eV, a phonon dispersion spectrum with no instabilities, and a 2-D Young's modulus and Poisson's ratio stiffer than those for graphane—the parent material for hydroxygraphane. Hence, hydroxygraphane has the desired electronic and mechanical properties to make it a viable candidate for a proton exchange membrane material capable of operating under anhydrous or low-humidity conditions.

### Graphical TOC Entry



Proton conduction is of fundamental importance in fields as diverse as cell function, <sup>1,2</sup> photosynthesis, <sup>3,4</sup> enzyme catalysis, <sup>5</sup> and battery and fuel cell technologies. <sup>6–9</sup> Proton transport in aqueous systems has been widely investigated through theoretical <sup>10,11</sup> and experimental techniques <sup>11,12</sup> for decades and is still an active area of research, as seen from recent intriguing findings of proton transport for water dissociation in nanoconfined channels <sup>13,14</sup> and unusual proton transport characteristics at the temperature of maximum density. <sup>15</sup> In contrast, the study of of proton transport under anhydrous conditions has not been studied as extensively. <sup>16</sup>

Proton exchange membrane (PEM) fuel cells are increasingly important in applications such as fuel cell vehicles and portable power generation. 17 Limitations of current PEM fuel cells include the requirement that the operating temperature not exceed about 80°C and that the membrane be sufficiently hydrated. Both of these requirements are the result of materials property limitations of the polymer electrolyte membrane, Nafion, 18 used in the current generation of fuel cells. The fundamental issue is that Nafion is not an intrinsic proton conduction material—it is only capable of conducting protons when sufficiently hydrated. There are significant advantages to increasing the operating temperature of PEM fuel cells and eliminating the need for membrane humidification, including increased kinetic rates, the availability of higher quality waste heat, higher resistance to electrode poisoning, and simplified water management. 16,19,20 Hence, there is a need to develop new materials that facilitate proton transport under anhydrous or low humidity conditions. 21,22

Recent work has focused on the discovery and synthesis of new materials capable of proton conduction under low-humidity or anhydrous conditions. <sup>23–30</sup> Porous metal organic frameworks and related materials have been proposed as Nafion replacements. <sup>22,24,27,28,31–35</sup> However, most of these materials have conductivities that are lower than Nafion or require water to be bound to the porous structure to facilitate proton conduction. <sup>28</sup> Even materials that have

high intrinsic proton conductivity have high resistance to conduction across grain boundaries and could suffer from stability issues. Hence, there is still a need to both understand proton conduction under anhydrous conditions and to develop materials that have higher conductivity and stability than those now available.

In this letter we show that graphane (an sp<sup>3</sup> hydrogenated version of graphene<sup>36</sup>) that is functionalized with hydroxyl groups, which is known as graphanol or hydroxygraphane,<sup>37</sup> has the potential to conduct protons via a Grotthuss-like mechanism<sup>38</sup> in the complete absence of water. We have used density functional theory (DFT) to study proton conduction on hydroxygraphane—a quasi two-dimensional (2-D) material constructed by replacing all the hydrogen atoms on one side of graphane with hydroxyl groups (OH), <sup>39</sup> as shown in Figure 1. We note that hydroxygraphane has been reported to be thermodynamically stable, according to ab-initio calculations. 40 More importantly, synthesis of hydroxygraphane has been reported, based on hydroboration of graphane oxide, <sup>37</sup> yielding stoichiometric ratios of OH and H groups.

We note that there have been two experimental reports in the literature of proton conduction on graphene oxide (GO). 41,42 Karim et al. 42 found that GO conducts protons on the surface when humidified. They hypothesize that protons are conducted through a hydrogen bonded network of water adsorbed on the surface. This work supports our hypothesis that a hydrogen bonded network on the surface of graphene-related materials will facilitate the conduction of protons. Cao et al. 41 demonstrated that sulfonated GO nanosheets can be used to create three-dimensional networks when integrated with Nafion to form a polymer matrix. This composite material was found to conduct protons at rates comparable with Nafion. Cao and co-workers posit that the sulfonate groups favor formation of well-connected water channels. Neither of these materials can conduct protons at low humidity because they lack a sufficient density of hydrogen bonding groups on the surface to create a contiguous network of hydrogen bonds. In related work, Bagusetty

et al. have predicted that graphane functionalized with a 1-D chain of hydroxyl groups can conduct protons under anhydrous conditions at appreciable rates. 43 However, this hypothetical material has not been made and is probably very difficult to make. Moreover, a single defect (e.g., a single missing OH group) will completely block proton conductivity along the 1-D chain. 43 Hydroxygraphane, in contrast, has been synthesized<sup>37</sup> and because the OH groups form a 2-D network of contiguous hydrogen bonds across the surface, <sup>39</sup> it should exhibit robust proton conductivity with respect to defects such as missing OH groups or carbon atoms. Hydroxygraphane also features a key descriptor for the facile conduction of protons, namely, an ordered and consistent distance between donor and acceptor (OH) groups of the hydrogen bonds, which was reported to enhance proton diffusivity in comparison to tortuous and amorphous morphologies present in most polymer electrolyte membranes. 44,45

successful synthesis of hydroxygraphane<sup>37</sup> suggests that it is possible to experimentally test this material for proton conduction. Before doing so, it is highly advantageous to use atomistic simulations to identify the potential for hydroxygraphane to function as a PEM material. Some of the requirements that an effective intermediate temperature PEM material must have are: (1) an ability to conduct protons at acceptably high rates over a range of temperatures, even in the absence of water; (2) electrical insulation, i.e., it must be a wide bandgap semiconductor; (3) mechanical robustness. It is the aim of this letter to evaluate in silico the suitability of hydroxygraphane with respect to these three criteria.

Computational Methodology. Our calculations were carried out with DFT methods as implemented in the Vienna ab-initio simulation package (VASP).  $^{46-48}$  The structural relaxation of the supercell shown in Figure 1 gave lattice parameters of: a=10.703 Å, b=8.027 Å, c=20.0 Å,  $\alpha=\beta=90^{\circ}$ ,  $\gamma=120^{\circ}$ . Projector augmented-wave (PAW) pseudopotentials  $^{49}$  were employed to describe the interactions between valence electrons and frozen cores. A kinetic energy cutoff for the plane-

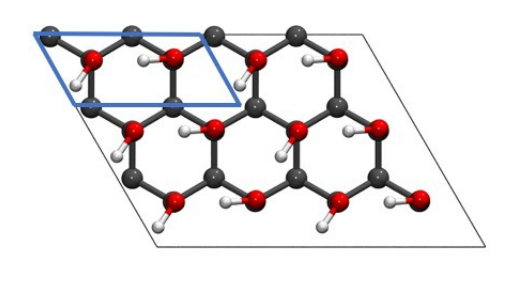




Figure 1: Top and side view of hydroxy-graphane in the herringbone configuration (carbons in gray, oxygens in red, hydrogens in white). The primitive cell (containing 10 atoms) is shown by the solid blue lines. Solid black lines show the supercell which is a  $3 \times 2$  replication of the primitive cell.

wave expansion was set to 520 eV and total energy convergence for self-consistent field calculations was set to  $10^{-9}$  eV to attain sufficient accuracy. The generalized gradient approximation exchange-correlation (XC) functional of Perdew-Burke-Ernzerhof (PBE) was used. <sup>50,51</sup> The Brillouin zone sampling was performed using a Monkhorst-Pack k-point grid size of 7 ×  $7 \times 1$ . All the ionic positions were relaxed until the forces were less than the tolerance of 10<sup>-3</sup> eV/Å. A vacuum spacing of 20 Å in the direction perpendicular to the surface of hydroxygraphane was employed to mitigate the interactions between the layers under periodic boundary conditions. The calculated bond lengths for C—C, C—H, C—O were found to be 1.57 Å, 1.11 Å and 1.43 Å, respectively, for the optimized configuration in Figure 1. These values agree well with those reported by Wang et al. 39

Proton mobility was assessed by examining proton mean square displacements, which were computed from a set of ten independent Born-Oppenheimer ab initio molecular dynamics (AIMD) simulations. These were performed on a  $2 \times 2 \times 1$  configuration of the system shown in Figure 1 having one excess proton, such that the system has an overall charge of +1 e. The average temperature of the simulations was about 800 K. Simulation details are

given in the Supporting Information.

Calculations performed using DFT charged systems under periodic boundary conditions impose an artificial counter-charge jellium background, which results in an error. 52 Bagusetty et al. 43 showed that this background charge error is not significant for computing the diffusion barriers for a similar charged system of 1-D hydroxylated graphane by comparing results with and without density-countercharge corrections.<sup>53</sup> Their results imply that background charge errors will be small for our system as well. We also note that quantum effects such as diffraction and proton tunneling are neglected in this study. Based on previous work, <sup>43</sup> we estimate that proton conduction rates will increase significantly when quantum diffraction is accounted for, but that proton tunneling will have a negligible impact.

The Heyd-Scuseria-Ernzerhorf (HSE06) short-range screened hybrid functional  $^{54,55}$  was used for accurate band structure calculations because the PBE functional is known to underestimate the bandgap of semiconductors. We have evaluated the structural stability by exploring the harmonic phonon dispersion spectrum computed using the PHONOPY software package  $^{56}$  in conjunction with VASP. The phonon calculations were carried out on a  $3 \times 3 \times 1$  supercell (containing 90 atoms) constructed from the primitive cell configuration shown in Figure 1.

Dynamics of Proton Conduction. We investigated the dynamic stability and proton conduction ability of hydroxygraphane containing one excess proton (H<sup>+</sup>) by performing AIMD simulations at high temperatures (about 800 K). We observed that hydroxygraphane with an excess proton is stable (or at least metastable) because aside from proton hopping, no bond breaking events of the underlying structure were observed in any of the ten independent simulations at 800 K. Our analysis of the AIMD trajectories indicated that proton conduction occurs by hopping of an excess proton from one OH group to the next over a 2-D network of hydrogen bonds. We noted that the hydroxyl groups surrounding the center of excess charge (i.e., OH group with an excess proton) reorient

themselves to accommodate the local changes made to the morphology due to the presence of the excess proton. The key to facile intrinsic proton conduction is the presence of a contiguous network of hydrogen bonds having an appropriate hydrogen bonding distance across the hydroxygraphane surface, coupled with the ability of the OH groups to rotate. 45,57 We observed that proton conduction on hydroxygraphane takes place through a Grotthuss-like mechanism, where a proton is transferred from one OH group to another, followed by a different H<sup>+</sup> moving to the next OH group, as illustrated in Figure 2. The mechanism of proton conduction is associated with a slight reorientation of the hydroxyl groups surrounding the excess charge, resulting in a reconfiguration of the hydrogen bonding network.

The proton mobility was quantified from the mean squared displacement (MSD) averaged over x and y directions along the plane of hydroxygraphane. The profile of MSD as a function of time at 800 K is plotted in Figure 3.

We have estimated the mean value of the selfdiffusion coefficient from the MSD profile using the Einstein relation. Our computed value is  $D = 1.1 \times 10^{-5} \text{ cm}^2/\text{s}$  with an uncertainty of  $\pm 2.6 \times 10^{-6}$  cm<sup>2</sup>/s (twice the standard deviation). For comparison, the value of D for 1-D hydroxylated graphane at 800 K is  $1.56 \times 10^{-4}$ cm<sup>2</sup>/s. <sup>43</sup> The observed reduction in the proton mobility is expected in going from a 1-D chain of hydroxylated graphane to a 2-D network in hydroxygraphane, and is due to the difference in the hydrogen bonding topology. There is a maximum of two hydrogen bonds (one donor and one acceptor) on any given OH group on 1-D hydroxylated graphane because there are only two neighboring OH groups. However, any OH group on hydroxygraphane has a coordination of six neighboring OH groups to which it can hydrogen bond. Hence, any given OH group could have three hydrogen bonds, one donor and two acceptors, and therefore the energy required to rotate an OH group is, on average, significantly higher than for the 1-D sys-

Another difference between the 1-D hydroxylated graphane and 2-D hydroxygraphane cases

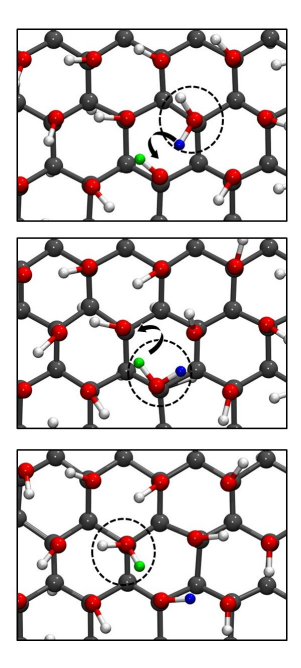


Figure 2: Snapshots of a proton conduction event in protonated hydroxygraphane from AIMD simulations at 800 K. An excess proton associated with a hydroxyl group is marked with a dashed circle to indicate the charge center. Protons participating in the conduction event are colored blue and green to aid in visualization. Hopping of these protons illustrate a Grotthuss-like mechanism (atom colors defined in Figure 1).

is that protons can obviously only diffuse along the 1-D chain of OH groups in the former, but protons can diffuse in any direction on the hydroxygraphane surface. Indeed, our MSD data show that proton mobility in the x and y directions is statistically equivalent, as can be seen from Figure 3(b). Hence, hydroxygraphane having defects (e.g., missing OH groups or missing C atoms) will still conduct protons, whereas a missing OH group on 1-D hydroxylated graphane will result in a complete blockage of proton conduction.  $^{43}$ 

The purpose of this paper is to establish that proton conduction does occur on hydroxygraphane, and to explore its mechanical and electronic properties. This paper does not attempt to fully characterize the diffusion coefficients and the corresponding conductivities, which can be determined from the Einstein relation and Nernst-Einstein equation, <sup>58</sup> respectively. We will explore the temperature dependence of diffusivity and conductivity at longer time scales and with higher statistical precision in a future paper.

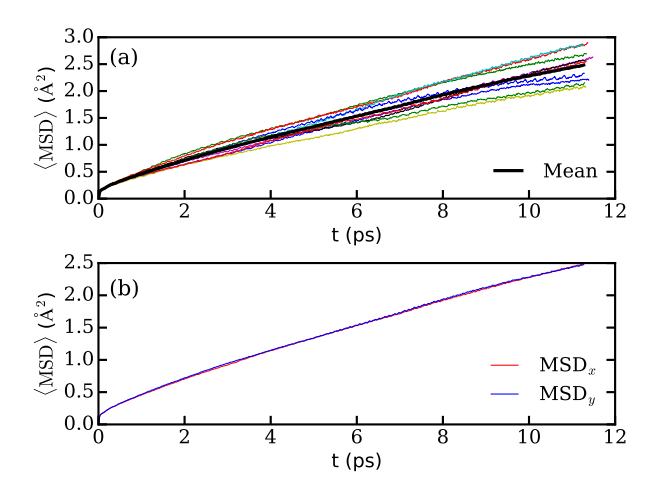


Figure 3: (a) Profiles of proton mean squared displacement as a function of time for hydroxygraphane with an excess proton at an average temperature of about 800 K. Thin lines in various colors are results from each of the ten uncorrelated simulations. The mean MSD profile is shown as the thick black curve. (b) Contributions of the proton MSD in x and y directions.

Electronic Properties. It is an obvious requirement that PEM materials be electronically insulating. We have computed the bandgap of

hydroxygraphane using four different exchangecorrelation functionals. We compared results from the PBE<sup>50,51</sup> semi-local generalized gradient functional and three hybrid functionals, HSE06, 54,55 PBE0, 59 and B3LYP, 60 which include different amounts of Hartree-Fock (HF) exchange. Results of these calculations are shown in Table 1. As expected, the bandgap predicted from PBE is significantly smaller than values computed from the hybrid functionals. We believe that the HSE06 functional is the most accurate of the exchange-correlation functionals we tested because it is known to be accurate for semiconductors. 61 The larger bandgap computed from PBE0 is likely a result of using a larger amount (25%) of full-range HF exchange, in comparison to B3LYP, which has 20% full-range HF exchange and HSE06 with 25% short-range HF exchange.

The band structure for hydroxygraphane computed from the HSE06 functional is shown in Figure 4. We see from this figure that the bandgap is direct and is located at the  $\Gamma$  point. We note that the band gap reported by Wang *et al.* computed from the PBE functional is about 1 eV larger than our PBE value.

Table 1: Values of the bandgap of hydroxygraphane computed from various exchange-correlation (XC) functionals

XC functional	Bandgap (eV)
PBE	2.23
HSE06	3.43
PBE0	4.10
B3LYP	3.11

One might expect that an excess proton added to hydroxygraphane would create a localized charge center, i.e., one H atom bound to a hydroxyl group could be identified as the "proton" and would have a significantly larger positive charge than the rest of the H atoms bound to other OH groups. We have tested this hypothesis by computing the charge on each atom of hydroxygraphane with a single added proton using the Density Derived Electrostatic and Chemical (DDEC6) charge analysis approach. <sup>62,63</sup> We found that the charges on H atoms bound to OH groups are all very sim-

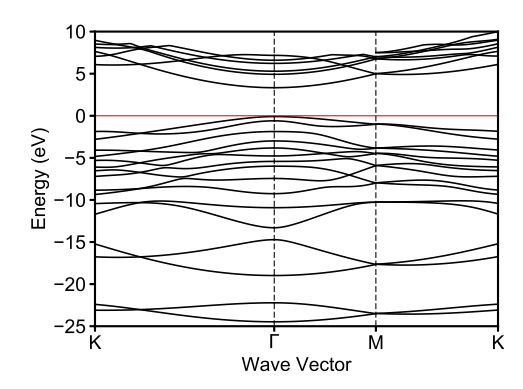


Figure 4: HSE06 electronic band structure of hydroxygraphane along a high-symmetry path. The Fermi level is shifted to zero energy and represented by a horizontal red line.

ilar, indicating that the excess proton is fairly delocalized (see Figure S2 and Tables S1 and S2 of the Supporting Information). This delocalization of the charge is consistent with our observation of a Grotthuss-like proton conduction mechanism. This is similar to the case for 1-D hydroxylated graphane <sup>43</sup> and for graphamine. <sup>64</sup>

We have computed phonon dispersion curves using the finite-displacement method <sup>56</sup> to investigate the stability of hydroxygraphane (see Figure S3 in the Supporting Information). Instabilities in the form of soft modes (modes with imaginary frequencies) were not found along any high-symmetry direction of the Brillouin zone under the harmonic approximation. The lack of soft modes indicates that hydroxygraphane is mechanically stable.

Elastic Properties. The elastic properties were investigated to provide insights into the mechanical rigidity of the hydroxygraphane. We have computed the in-plane Young's modulus Y, which is a 2-D version of Young's modulus, for hydroxygraphane as described in the Supporting Information. These calculations gave  $Y = 252 \text{ J/m}^2$ . For comparison, this value of Y falls in-between the reported values for chair graphane  $(243 \text{ J/m}^2)^{65,66}$  and graphene  $(340 \pm 50 \text{ J/m}^2)$ . The increase in Y for hydroxygraphane relative to chair graphane is the result of the 2-D network of hydrogen bonds on the surface of hydroxygraphane, which provides resistance to in-plane stretching and compression. We have also computed Poisson's ratio  $\nu$ for hydroxygraphane as described in the Supporting Information. Our computations gave  $\nu=0.11$ , which is comparable to graphene  $(\nu=0.16)^{67}$  and almost double that of the parent material, chair graphane  $(\nu=0.07).^{65}$  Our computed values of Y and  $\nu$  for hydroxygraphane indicate that it has reasonable mechanical properties for a PEM material.

We have demonstrated in silico that hydroxygraphane is an intrinsic proton conduction material, capable of conducting protons anhydrously through a Grotthuss-like mechanism, whereby a proton hops from one OH group to another, followed by a different proton hopping to a third neighboring OH group. is the contiguous network of hydrogen bonds on the surface of hydroxygraphane that provides the necessary pathways for proton transport. We believe that proton conduction will occur through a similar mechanism for any surface having a network of hydrogen bonded moieties, even in the complete absence of water. Importantly, morphological defects, such as the absence of one or more adjacent hydroxyl groups, will have a minor impact on proton conduction because of the presence of redundant percolating hydrogen bonding pathways. Our DFT calculations provide evidence that hydroxygraphane has the requisite electronic and mechanical properties for making a practical proton exchange membrane material capable of operating at intermediate temperatures and low humidities. Given the recently reported synthesis of hydroxygraphane, <sup>37</sup> our work provides strong motivation to experimentally test our predictions of anhydrous proton transport.

#### Conflicts of interest

The authors declare no competing financial interest.

## Acknowledgments

This work was supported by National Science Foundation under Award No. CBET 1703266. This work used the Extreme Science and Engineering Discovery Environment

(XSEDE), which is supported by National Science Foundation grant number ACI-1548562, under allocation No. TG-DMR110091. Computational resources were also provided by the Center for Research Computing at the University of Pittsburgh.

#### References

- (1) Hirst, J. Mitochondrial Complex I. *Annu. Rev. Biochem.* **2013**, *82*, 551–575.
- (2) Cheng, S. Y.; Leonard, J. L.; Davis, P. J. Molecular aspects of thyroid hormone actions. *Endocr. Rev.* **2010**, *31 2*, 139–70.
- (3) Armbruster, U.; Galvis, V. C.; Kunz, H.-H.; Strand, D. D. The regulation of the chloroplast proton motive force plays a key role for photosynthesis in fluctuating light. *Curr. Opin. Plant Biol.* **2017**, *37*, 56 62.
- (4) Vinyard, D. J.; Ananyev, G. M.; Charles Dismukes, G. Photosystem II: The Reaction Center of Oxygenic Photosynthesis. *Annu. Rev. Biochem.* **2013**, *82*, 577–606.
- (5) Paul, S.; Paul, T. K.; Taraphder, S. Reaction Coordinate, Free Energy, and Rate of Intramolecular Proton Transfer in Human Carbonic Anhydrase II. J. Phys. Chem. B. 2018, 122, 2851–2866.
- (6) Kusoglu, A.; Weber, A. Z. New Insights into Perfluorinated Sulfonic-Acid Ionomers. *Chem. Rev.* **2017**, *117*, 987–1104.
- (7) Shin, D. W.; Guiver, M. D.; Lee, Y. M. Hydrocarbon-Based Polymer Electrolyte Membranes: Importance of Morphology on Ion Transport and Membrane Stability. Chem. Rev. 2017, 117, 4759–4805.
- (8) Kreuer, K.-D. Proton Conductivity: Materials and Applications. *Chem. Mater.* **1996**, *8*, 610–641.
- (9) Lototskyy, M. V.; Tolj, I.; Davids, M. W.; Klochko, Y. V.; Parsons, A.;

- Swanepoel, D.; Ehlers, R.; Louw, G.; van der Westhuizen, B.; Smith, F. et al. Metal hydride hydrogen storage and supply systems for electric forklift with low-temperature proton exchange membrane fuel cell power module. *Int. J. Hydrog. Energy* **2016**, *41*, 13831–13842.
- (10) Marx, D. Proton Transfer 200 Years after von Grotthuss: Insights from Ab Initio Simulations. ChemPhysChem 2006, 7, 1848–1870.
- (11) Agmon, N.; Bakker, H. J.; Campen, R. K.; Henchman, R. H.; Pohl, P.; Roke, S.; Thämer, M.; Hassanali, A. Protons and Hydroxide Ions in Aqueous Systems. *Chem. Rev.* **2016**, *116*, 7642–7672.
- (12) Wolke, C. T.; A.; Fournier, J. C.; Dzugan, L. Fagiani, Μ. R.; Odbadrakh, T. T.; Knorke, H.; Jordan, K. D.; McCoy, A. B.; Asmis, K. R.; Johnson, M. A. Spectroscopic snapshots of the proton-transfer mechanism water. Science **2016**, 354, 1131–1135.
- (13) Muñoz Santiburcio, D.; Marx, D. Nanoconfinement in Slit Pores Enhances Water Self-Dissociation. *Phys. Rev. Lett.* **2017**, *119*.
- (14) Sirkin, Y. A. P.; Hassanali, A.; Scherlis, D. A. One-Dimensional Confinement Inhibits Water Dissociation in Carbon Nanotubes. J. Phys. Chem. Lett 2018, 9, 5029–5033.
- (15) Silletta, E. V.; Tuckerman, M. E.; Jerschow, A. Unusual Proton Transfer Kinetics in Water at the Temperature of Maximum Density. *Phys. Rev. Lett.* **2018**, *121*.
- (16) Schuster, M. F.; Meyer, W. H. Anhydrous Proton-Conducting Polymers. *Annu. Rev. Mater. Res.* **2003**, *33*, 233–261.
- (17) Wee, J.-H. Applications of proton exchange membrane fuel cell systems. *Renew. Sust. Energy. Rev.* **2007**, *11*, 1720–1738.

- (18) Mauritz, K. A.; Moore, R. B. State of Understanding of Nafion. *Chem. Rev.* **2004**, *104*, 4535–4586.
- (19) Zhang, J.; Xie, Z.; Zhang, J.; Tang, Y.; Song, C.; Navessin, T.; Shi, Z.; Song, D.; Wang, H.; Wilkinson, D. P. et al. High temperature PEM fuel cells. J. Power Sources 2006, 160, 872–891.
- (20) Steele, B. C. H.; Heinzel, A. Materials for fuel-cell technologies. *Nature* 2001, 414, 345–352.
- (21) Park, J.-S.; Shin, M.-S.; Kim, C.-S. Proton exchange membranes for fuel cell operation at low relative humidity and intermediate temperature: An updated review. *Curr. Opin. Electrochem.* **2017**, *5*, 43–55.
- (22) Ramaswamy, P.; Wong, N. E.; Shimizu, G. K. H. MOFs as proton conductors challenges and opportunities. *Chem. Soc. Rev.* 2014, 43, 5913.
- (23) Paddison, S. Proton Conduction Mechanisms at Low Degrees of Hydration in Sulfonic Acid-Based Polymer Electrolyte Membranes. *Annu. Rev. Mater. Sci.* **2003**, *33*, 289.
- (24) Chandra, S.; Kundu, T.; Kandambeth, S.; BabaRao, R.; Marathe, Y.; Kunjir, S. M.; Banerjee, R. Phosphoric Acid Loaded Azo (-N = N-) Based Covalent Organic Framework for Proton Conduction. J. Am. Chem. Soc. 2014, 136, 6570.
- (25) Luo, H.-B.; Wang, M.; Zhang, J.; Tian, Z.-F.; Zou, Y.; Ren, X.-M. Open-Framework Chalcogenide Showing Both Intrinsic Anhydrous and Water-Assisted High Proton Conductivity. ACS Appl. Mater. Interfaces 2018, 10, 2619–2627.
- (26) Inukai, M.; Horike, S.; Itakura, T.; Shinozaki, R.; Ogiwara, N.; Umeyama, D.; Nagarkar, S.; Nishiyama, Y.; Malon, M.; Hayashi, A. et al. Encapsulating Mobile Proton Carriers into Structural Defects in Coordination Polymer Crystals: High Anhydrous Proton Conduction and Fuel Cell

- Application. J. Am. Chem. Soc. 2016, 138, 8505–8511.
- (27) Shimizu, G. K. H.; Taylor, J. M.; Kim, S. Proton Conduction with Metal-Organic Frameworks. *Science* **2013**, *341*, 354.
- (28) Horike, S.; Umeyama, D.; Kitagawa, S. Ion Conductivity and Transport by Porous Coordination Polymers and Metal-Organic Frameworks. *Acc. Chem. Res.* **2013**, *46*, 2376–2384.
- (29) Vilčiauskas, L.; Tuckerman, M. E.; Bester, G.; Paddison, S. J.; Kreuer, K.-D. The mechanism of proton conduction in phosphoric acid. *Nat. Chem.* **2012**, 4, 461–466.
- (30) Hurd, J. A.; Vaidhyanathan, R.; Thangadurai, V.; Ratcliffe, C. I.; Moudrakovski, I. L.; Shimizu, G. K. H. Anhydrous proton conduction at 150 ° C in a crystalline metal-organic framework. *Nat. Chem.* **2009**, *1*, 705–710.
- (31) Li, A.-L.; Gao, Q.; Xu, J.; Bu, X.-H. Proton-conductive metal-organic frameworks: Recent advances and perspectives. *Coord. Chem. Rev.* **2017**, *344*, 54 82.
- (32) Yoon, M.; Suh, K.; Kim, H.; Kim, Y.; Selvapalam, N.; Kim, K. High and Highly Anisotropic Proton Conductivity in Organic Molecular Porous Materials. *Angew. Chem. Int. Ed.* **2011**, *50*, 7870–7873.
- (33) Nagarkar, S. S.; Unni, S. M.; Sharma, A.; Kurungot, S.; Ghosh, S. K. Two-in-One: Inherent Anhydrous and Water-Assisted High Proton Conduction in a 3D Metal-Organic Framework. *Angew. Chem.* **2013**, 126, 2676.
- (34) Peng, Y.; Xu, G.; Hu, Z.; Cheng, Y.; Chi, C.; Yuan, D.; Cheng, H.; Zhao, D. Mechanoassisted Synthesis of Sulfonated Covalent Organic Frameworks with High Intrinsic Proton Conductivity. ACS Appl. Mater. Interfaces 2016, 8, 18505.

- (35) Ramaswamy, P.; Wong, N. E.; Gelfand, B. S.; Shimizu, G. K. H. A Water Stable Magnesium MOF That Conducts Protons over 10<sup>-2</sup> S cm<sup>-1</sup>. *J. Am. Chem. Soc.* **2015**, *137*, 7640.
- (36) Sofo, J. O.; Chaudhari, A. S.; Barber, G. D. Graphane: A two-dimensional hydrocarbon. *Phys. Rev. B.* **2007**, *75*, 153401.
- (37) Poh, H. L.; Sofer, Z.; Šimek, P.; Tomandl, I.; Pumera, M. Hydroboration of Graphene Oxide: Towards Stoichiometric Graphol and Hydroxygraphane. *Chem. Eur. J.* **2015**, *21*, 8130–8136.
- (38) Agmon, N. The Grotthuss mechanism. *Chem. Phys. Lett.* **1995**, *244*, 456–462.
- (39) Wang, W. L.; Kaxiras, E. Graphene Hydrate: Theoretical Prediction of a New Insulating Form of Graphene. *New J. Phys.* **2010**, *12*, 125012.
- (40) Buonocore, F.; Capasso, A.; Lisi, N. An ab initio study of hydroxylated graphane. J. Chem. Phys. **2017**, 147, 104705.
- (41) Cao, L.; Wu, H.; Yang, P.; He, X.; Li, J.; Li, Y.; Xu, M.; Qiu, M.; Jiang, Z. Graphene Oxide-Based Solid Electrolytes with 3D Prepercolating Pathways for Efficient Proton Transport. Adv. Funct. Mater. 2018, 1804944.
- (42) Karim, M. R.; Hatakeyama, K.; Matsui, T.; Takehira, H.; Taniguchi, T.; Koinuma, M.; Matsumoto, Y.; Akutagawa, T.; Nakamura, T.; Noro, S.-i. et al. Graphene Oxide Nanosheet with High Proton Conductivity. J. Am. Chem. Soc. **2013**, 135, 8097–8100.
- (43) Bagusetty, A.; Choudhury, P.; Saidi, W. A.; Derksen, B.; Gatto, E.; Johnson, J. K. Facile Anhydrous Proton Transport on Hydroxyl Functionalized Graphane. *Phys. Rev. Lett.* **2017**, *118*, 186101.

- (44) Trigg, E. B.; Gaines, T. W.; Maréchal, M.; Moed, D. E.; Rannou, P.; Wagener, K. B.; Stevens, M. J.; Winey, K. I. Self-assembled highly ordered acid layers in precisely sulfonated polyethylene produce efficient proton transport. *Nat. Mater.* 2018, 17, 725–731.
- (45) Umeyama, D.; Horike, S.; Inukai, M.; Itakura, T.; Kitagawa, S. Inherent Proton Conduction in a 2D Coordination Framework. J. Am. Chem. Soc. 2012, 134, 12780–12785.
- (46) Kresse, G.; Hafner, J. Ab Initio Molecular Dynamics for Liquid Metals. *Phys. Rev.* B. 1993, 47, 558–561.
- (47) Kresse, G.; Furthmüller, J. Efficient Iterative Schemes for Ab Initio Total-Energy Calculations Using a Plane-Wave Basis Set. *Phys. Rev. B.* **1996**, *54*, 11169–11186.
- (48) Kresse, G.; Furthmüller, J. Efficiency of Ab-Initio Total Energy Calculations for Metals and Semiconductors Using a Plane-Wave Basis Set. Comput. Mater. Sci. 1996, 6, 15–50.
- (49) Kresse, G.; Joubert, D. From Ultrasoft Pseudopotentials To the Projector Augmented-Wave Method. *Phys. Rev. B.* **1999**, *59*, 1758–1775.
- (50) Perdew, J. P.; Burke, K.; Ernzerhof, M. Generalized Gradient Approximation Made Simple. Phys. Rev. Lett. 1996, 77, 3865–3868.
- (51) Zhang, Y.; Yang, W. Comment on "Generalized Gradient Approximation Made Simple". *Phys. Rev. Lett.* **1998**, *80*, 890–890.
- (52) Makov, G.; Payne, M. C. Periodic Boundary Conditions in Ab Initio Calculations. *Phys. Rev. B.* **1995**, *51*, 4014–4022.
- (53) Dabo, I.; Kozinsky, B.; Singh-Miller, N. E.; Marzari, N. Electrostatics in Periodic Boundary Conditions and Real-Space Corrections. *Phys. Rev. B.* 2008, 77, 115139.

- (54) Heyd, J.; Scuseria, G. E.; Ernzerhof, M. Hybrid functionals based on a screened Coulomb potential. *J. Chem. Phys.* **2003**, 118, 8207.
- (55) Heyd, J.; Scuseria, G. E.; Ernzerhof, M. Erratum: "Hybrid functionals based on a screened Coulomb potential" [J. Chem. Phys. 118, 8207 (2003)]. J. Chem. Phys. 2006, 124, 219906.
- (56) Togo, A.; Tanaka, I. First principles phonon calculations in materials science. *Scr. Mater.* **2015**, *108*, 1–5.
- (57) Nagamani, C.; Viswanathan, U.; Versek, C.; Tuominen, M. T.; Auerbach, S. M.; Thayumanavan, S. Importance of dynamic hydrogen bonds and reorientation barriers in proton transport. Chem. Commun. 2011, 47, 6638.
- (58) Prentice, G. Electrochemical Engineering Principles; Prentice-Hall International Se; Prentice Hall, 1991.
- (59) Adamo, C.; Barone, V. Toward reliable density functional methods without adjustable parameters: The PBE0 model. *J. Chem. Phys.* **1999**, *110*, 6158–6170.
- (60) Stephens, P. J.; Devlin, F. J.; Chabalowski, C. F.; Frisch, M. J. Ab Initio Calculation of Vibrational Absorption and Circular Dichroism Spectra Using Density Functional Force Fields. J. Phys. Chem. 1994, 98, 11623–11627.
- (61) Garza, A. J.; Scuseria, G. E. Predicting Band Gaps with Hybrid Density Functionals. J. Phys. Chem. Lett. 2016, 7, 4165.
- (62) Manz, T. A.; Limas, N. G. Introducing DDEC6 atomic population analysis: part 1. Charge partitioning theory and methodology. RSC Adv. 2016, 6, 47771– 47801.
- (63) Limas, N. G.; Manz, T. A. Introducing DDEC6 Atomic Population Analysis: Part 2. Computed Results for a Wide Range of Periodic and Nonperiodic Materials. RSC Adv. 2016, 6, 45727.

- (64) Bagusetty, A.; Livingston, J.; Johnson, J. K. *J. Phys. Chem. C* **2018**, under review.
- (65) Topsakal, M.; Cahangirov, S.; Ciraci, S. The Response of Mechanical and Electronic Properties of Graphane To the Elastic Strain. *Appl. Phys. Lett.* **2010**, *96*, 091912.
- (66) Cadelano, E.; Palla, P. L.; Giordano, S.; Colombo, L. Elastic properties of hydrogenated graphene. *Phys. Rev. B.* **2010**, *82*, 235414.
- (67) Lee, C.; Wei, X.; Kysar, J. W.; Hone, J. Measurement of the Elastic Properties and Intrinsic Strength of Monolayer Graphene. *Science* **2008**, *321*, 385.